Energy & Buildings 228 (2020) 110445

Contents lists available at ScienceDirect

Energy & Buildings

journal homepage: www.elsevier.com/locate/enb

Cluster analysis-based anomaly detection in building automation systems

H. Burak Gunay *, Zixiao Shi [1]

Department of Civil and Environmental Engineering, Carleton University, Ottawa, Canada

ARTICLE INFO

Article history:
Received 16 May 2020
Revised 30 July 2020
Accepted 30 August 2020
Available online 6 September 2020

Keywords:
Anomaly detection
Building automation system
Cluster analysis
Variable air volume terminal units
Air handling units

ABSTRACT

Faults in heating, ventilation, and air-conditioning control networks substantially affect energy and comfort performance in commercial buildings. As these control networks are comprised of many sensors and actuators, it is challenging to identify, often subtle, anomalies caused by these faults. In this paper, we develop a cluster analysis method for anomaly detection. The proposed method consolidates the building automation system data into a small number of distinct patterns of operation. These distinct patterns help energy managers discover and interpret anomalies through visualization of these patterns. The method was demonstrated with a year's worth of building automation system data from 247 thermal zones and an air handling unit. Anomalies associated with zone temperature and airflow control were identified in about one-third of these zones. At the air handling unit-level, we identified anomalies related with three different faults: the use of economizer mode with perimeter heating, and leaky outdoor and return air dampers. The use of economizer mode with perimeter heating affected 39% to 52% of the total operation period and caused the outdoor air damper to remain fully open and the heat recovery unit to remain off during most of the heating season.

1. Introduction

Heating, ventilation, and air-conditioning (HVAC) control systems in commercial and institutional buildings consist of a large network of sensors and actuators, which are often manually configured and commissioned after construction. Only rarely are they re-commissioned during occupancy. Consequently, faults in HVAC control systems remain invisible to energy managers and operators until occupant complaints trigger work-orders or a point-by-point inspection of the control network is carried out during re-commissioning [1]. These faults can be configurational mistakes arising from inappropriate setpoints and schedules (soft faults), or they can be hard faults due to failed devices such as sensors and actuators. Faults in large commercial and institutional buildings are estimated to waste 5% to 30% of the energy used by HVAC systems [2]; further, they deteriorate occupant comfort, and adversely affect workplace productivity and tenant satisfaction.

1.1. Background and previous work

Fault detection and diagnostics (FDD) techniques that rely on data from building automation systems (BAS) represent a major opportunity for the early detection of faults before they waste energy and cause discomfort. As documented in several recent reviews [3–5], a large body of literature has been dedicated to FDD in HVAC systems.

1.1.1. Overview of FDD methods

As proposed by Katipamula and Brambley [6,7], FDD methods for building HVAC systems can be grouped into three broad categories: qualitative, quantitative (i.e., whitebox, physics-based), and process history-based methods. The qualitative FDD methods are *if-then-else* statements formulated based on expert thresholds [8]. For example, one of the expert rules defined by Bruton et al. [9] was a check for deviations from an air handling unit's (AHU) supply air temperature and setpoint. Similarly, Schein et al. [10] developed 28 rules to diagnose common AHU faults such as stuck or leaking mixing box dampers, heating and cooling coil valves, temperature sensor faults, and controller programming errors related to tuning, setpoints, and sequencing logic. They tested these rules in a simulation-based investigation and a field study. Schein and House [11] also formulated rules for VAV terminal unit

* Corresponding author at: Carleton University, Department of Civil and Environmental Engineering, 1125 Colonel By Drive, Ottawa, Ontario K1S 5B6, Canada.
E-mail address: burakgunay@cunet.carleton.ca (H.B. Gunay).

[1] When this research was conducted, Zixiao Shi's primary affiliation was Construction Research Centre, National Research Council, Ottawa, Canada.

https://doi.org/10.1016/j.enbuild.2020.110445
0378-7788/

faults such as damper / reheat valves getting stuck at a certain position and faulty differential pressure sensors. These rules were based on cumulative sum (CUSUM) charts – which accumulate the error in meeting the airflow and temperature setpoints over time. They demonstrated this approach with a small number of artificially induced (through simulation and experiments) faults. Wang et al. [12] and Qin et al. [13] also used CUSUM charts for VAV terminal unit damper and airflow sensor faults, and inappropriate airflow and temperature setpoints. These two studies identified ten types of faults affecting VAV terminal units. Their field survey revealed that over 20% of the zones were suffering from at least one of these ten fault types. Other examples for qualitative FDD methods are the rules derived by Cho et al. [14] for VAV terminals and AHUs through transient pattern analysis, and Lauro et al. [15] and Lianzhong and Zaheeruddin [16] through fuzzy logic modelling.

Quantitative approaches rely on physics-based models to detect faults. For example, O'Neill et al. [17] developed a diagnostic method based on the building performance simulation tool EnergyPlus. They used the co-simulation environment BCVTB [18] to connect Matlab, EnergyPlus, and the BAS of a real building. Likely due to the engineering cost associated with developing physics-based models, examples of quantitative FDD approaches from the literature are scarce.

The third category is the process history based FDD approaches. Unlike qualitative and quantitative FDD approaches, process history-based approaches rely on long term data records [4]. With the widespread use of commercial BAS data archiving systems, recent efforts have been mostly dedicated to process history based FDD methods. Kim and Katipamula [4] report that nearly 90% of the process history based FDD methods employed blackbox models. For example, Wang et al. [19] employed regression models to compute performance indices for chillers, cooling towers, heat exchangers, and variable speed pumps – e.g., efficiency of a heat exchanger, coefficient of performance of a chiller. The residuals of these regression models were treated as symptoms to diagnose faults such as evaporator fouling, compressor degradation, condenser fouling, and refrigerant leakage. Yuwono et al. [20] employed a time-series modelling technique called auto-regressive neural networks for AHU faults by using the ASHRAE RP 1312 dataset [21]. Najafi et al. [22] also adopted a time-series modelling approach for AHU diagnostics. To estimate the mixed air temperature, they developed a model to remove the effect of heating and cooling coils on the supply air temperature by looking at coil valve positions at previous time lags. Thus, they were able to diagnose an outdoor air intake damper stuck fault by simply looking at the return and outdoor air temperatures. In another study, support vector machines were used to detect and diagnose two categories of chiller faults [23]. They investigated the viability of FDD algorithms for multiple-simultaneous faults affecting the same system. A few studies developed neural [24–26] and Bayesian network [27,28] models to detect and diagnose VAV and AHU faults.

Aside from the process history based FDD approaches employing blackbox models, a few studies employed greybox models to develop FDD algorithms for chillers [29] and VAV terminal units [30–32]. For example, Shi et al. [32] trained first-order thermal network models using data generated from EnergyPlus simulations. They used the model parameters together with dynamic Bayesian networks to diagnose faults induced into the EnergyPlus model.

1.1.2. Limitations of FDD methods

Despite these efforts, there are a few limitations related with the existing FDD methods:

- Limited transferability of the qualitative methods: Many of the existing commercial FDD solutions still rely on expert rules, which are known to generate many false positives and negatives due to the limited transferability of fault thresholds from one building to another [33].
- Lack of labelled data for training and validation of process history-based methods: A major limitation of the process history based FDD methods is their dependency on labelled data to train and validate an algorithm which can reliably distinguish faulty modes of operation from normal operation. In the reviewed literature, many researchers resorted to data sources generated from simulation tools or small-scale experiments instead of faults occurring naturally in-service. To our knowledge, there are only two public fault-symptom datasets emerging from ASHRAE RP 1020 and 1312 [21,34].
- Interpretability of faults by operations staff: Traditional AFDD tools fail to include operators in the decision-making process. Operators are prompted with alarms and provided with little context to engage in the process of addressing them. They are expected to manually investigate BAS trendlogs to verify and interpret alarms and determine the appropriate actions. As stated by Bruton et al. [9], operators are often overwhelmed by BAS data as the energy management systems fail to consolidate the data into a clear and coherent format. Furthermore, AFDD often fails to deprioritize false positives for trivial faults, which can lead to overwhelming amounts of alarms in a building [3].

1.1.3. Use of cluster analysis with FDD methods

While cluster analysis-based anomaly detection algorithms have been successfully employed on meter data to detect abnormalities in building energy use patterns [36–41], they have been seldom used with BAS data. For example, Narayanaswamy et al. [42] employed a method involving the k-means++ clustering algorithm [43] on 237 VAV terminal units in a large building and identified 78 anomalies. In another study, Du et al. [24] successfully employed subtractive clustering on features extracted through the principal component analysis to distinguish different fault categories among each other and from normal operation. Their focus was on supply air temperature sensor and controller, supply and return water temperature sensors, and coil valve faults in AHUs. Yan et al. [44] employed the density-based clustering algorithm OPTICS to detect sensor faults in AHUs. The effectiveness of their method was demonstrated on data collected from TRNSYS simulations. Lastly, Novikova et al. [45] also employed a density-based clustering algorithm (a modified version of DBSCAN) for anomaly detection on BAS data of a three-storey building. These studies have demonstrated that cluster analysis is an approach capable of consolidating large amount of BAS data into a small number of operational patterns [35]; thus, it is suitable for human-in-the-loop identification and interpretation of HVAC faults.

1.2. Objectives and document structure

Existing AFDD algorithms suffer from inaccuracies as they largely rely on expert rules instead of large verified fault-symptom datasets. Further, these algorithms generate alarms without providing any context to the operations staff. In this paper, we argue that operations staff needs to be actively involved in the decision-making process for the effective use of AFDD tools. To this end, the objective of this paper is not to introduce a new AFDD approach; instead, the paper introduces a novel cluster analysis method to consolidate a large BAS dataset to a small number of patterns so that operations staff can visually identify otherwise undetected issues and interpret those detected by existing AFDD tools. Simply put, this method is intended to identify distinct pat-

terns of operation to help energy managers discover and interpret anomalies.

To this end, the paper first presents the cluster analysis-based anomaly detection approach. Specifically, the features and algorithms employed to build and to evaluate the cluster models are presented. Subsequently, characteristics of the BAS dataset, which we used to demonstrate the anomaly detection method, are introduced. The results and discussion section applies the method to the BAS data from 247 VAV terminal units, 58 perimeter heaters, and an AHU with a heat recovery wheel (HRW). Note that our scope is limited to anomalies in VAV terminal units, perimeter heaters, and AHUs. Anomalies in other HVAC devices and systems are outside the scope of this paper.

2. Methodology

2.1. Background on cluster analysis

Before delving into the use of cluster analysis in the BAS anomaly detection problem, we will provide a brief introduction to clustering. Clustering is an unsupervised machine learning technique widely used to group unlabelled data into categories with shared characteristics. In our context, this implies grouping data from many subsystems of a building into a small number of similarly behaving categories or grouping data from a building system into a few modes of operation. In this paper, we will refer to the former as *spatial clustering*, whereas the latter will be referred to as *temporal clustering*.

Clustering algorithms can be broadly grouped into four categories: centroid-, connectivity-, density-, and distribution-based algorithms. Centroid-based clustering algorithms (e.g., k-means) iteratively search a user-defined number of cluster centers and associate data to the closest cluster centers such that the sum of intra-cluster variances is minimized. Connectivity-based clustering algorithms (i.e., hierarchical clustering) partition a dataset by using a linkage matrix that defines the dissimilarity of each data point with the rest of the dataset. Connectivity-based clustering algorithms generate a hierarchy of clusters that incorporate one another at different distance thresholds. Thus, they are often visualized using a dendrogram. Density-based clustering algorithms (e.g., DBSCAN [46]) search areas of high data density to form clusters. Similar to connectivity-based clustering algorithms, they form clusters by iteratively connecting a data point to the neighbouring data; however, the decision to connect is based on a user-defined distance threshold. Lastly, distribution-based clustering algorithms (e.g., Gaussian mixture models) iteratively fit a user-defined number of probability density functions to a dataset. A data point is then assigned to the most likely probability density function – representing a unique cluster.

Each clustering algorithm category offers certain benefits; thus, their appropriateness should be assessed for each unique scenario. In addition, clustering algorithms require user-defined hyperparameters, which ultimately affects the number and shape of clusters generated. Clustering algorithms and their hyperparameters can be evaluated by a cluster evaluation criterion such as the Calinski-Harabasz index [47]. The Calinski-Harabasz index is a metric to assess the quality of clustering results. It is a measure of the ratio of inter-cluster variances to intra-cluster variances, and it includes a penalty factor for the number of clusters to avoid overfitting. The number of clusters and algorithm category that result in the highest Calinski-Harabasz index value for a given dataset is considered the most appropriate and selected for analysis. Note that here we provided a brief introduction to clustering, detailed information on cluster analysis theory and application can be found elsewhere [48].

2.2. Cluster analysis method for anomaly detection

The cluster analysis is intended to be used with zone- and AHU-level time-series data from a BAS. The zone-level analysis uses four common data point types: temperature, temperature setpoint, airflow, and airflow setpoint. In addition, when available, data for perimeter heater (i.e., radiator) valve states are used.

The AHU-level analysis uses data from seven actuators and five sensors: outdoor and return air damper position ($S_{dp,oa}$ and $S_{dp,ra}$), heating and cooling coil valve state (S_{hc} and S_{cc}), humidifier valve state (S_h), supply fan state (S_{fan}), outdoor, return, and supply air temperature (T_{oa}, T_{ra}, T_{sa}), return air humidity (H_{ra}), and supply air pressure (P_{sa}). The average state of perimeter heaters (S_{rad}) is included to examine their causal relationship with an AHU's operation. Fig. 1 presents these data point types on a simple schematic diagram of a generic AHU with an HRW. Note that these are common data point types in many VAV zones and AHUs; and the method presented can also be applied to AHUs without HRWs and humidifiers.

Note that in a large commercial building, the method requires clustering a few data point types from many zones and many data point types from a small number of AHUs. Hence, zone-level clustering is intended to identify patterns of VAV and radiator operation across many zones, whereas AHU-level clustering is intended to identify an AHU's patterns of operation over a long period. The objective of the cluster analysis-based anomaly detection method is to consolidate the data (spatially for zones and temporally for AHUs) to a form that facilitates the detection of operational anomalies at the zone- and AHU-level.

Fig. 2 presents two pseudocodes illustrating the procedure to conduct this analysis. The zone-level analysis is carried out in eight steps Z1 to Z8, and the system-level analysis is carried out in four steps S1 to S4. The procedure involves three clustering methods for each step: k-means with squared Euclidean distances, hierarchical clustering by using Ward's linkage method with Euclidean distances, and Gaussian mixture model (GMM) clustering. At each step, the Calinski-Harabasz index [47] is computed by varying the number of clusters between two and ten and by using the three different clustering methods. In other words, the procedure employs three different clustering techniques and selects the best one automatically based on their ability to partition the features of a dataset into distinct groups, whereby distinctness is quantified based on the ratio of intra-cluster variance to the inter-cluster variance. The number of clusters and the algorithm that maximize the index for each step are selected. 12 Matlab functions for the eight zone-level and four system-level steps as well as sample data for these functions are included as supplemental files to this paper.

2.2.1. Zone-level anomaly detection

Zone-level anomaly detection involves an investigation of temperature and VAV airflow control errors – i.e., the differences between a setpoint and a manipulated variable. Fig. 3 presents an illustrative example of the temperature and airflow control errors in a zone over a day. The patterns of airflow and temperature control errors are studied in eight steps.

The first step involves (Z1 in Table 1) clustering the mean absolute temperature and airflow control errors during regular workhours (9 am to 5 pm on weekdays only). These two features are normalized to be between zero and one (i.e., min–max feature scaling) and then clustered. The intent of this first step is to isolate zones with large temperature or airflow control errors.

For the second step (Z2 in Table 1), a line-fit is trained between the temperature control error and the outdoor temperature during workhours. In this paper, we applied Z2 for each zone with a large temperature control error – as identified in step one. In practice, the cluster or clusters with large temperature control errors need

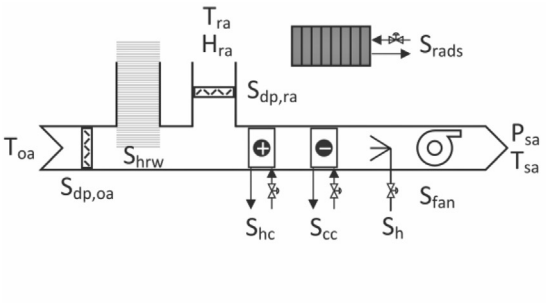

Symbol	Definition
T_{oa}	Outdoor temperature (°C)
$S_{dp,oa}$	Outdoor air damper (%)
S_{hrw}	State of HRW (%)
T_{ra}	Return air temperature (°C)
H_{ra}	Return air humidity (%)
$S_{dp,ra}$	Return air damper (%)
S_{hc}	Heating coil state (%)
S_{cc}	Cooling coil state (%)
S_{h}	Humidifier state (%)
S_{fan}	Supply fan state (%)
P_{sa}	Supply air pressure (Pa)
T_{sa}	Supply air temperature (°C)
S_{rads}	Fraction of radiators on (%)

Fig. 1. A schematic diagram presenting the AHU data for the anomaly detection method.

```
procedure: spatial clustering for zone-level data

input: temperature, temperature setpoint,
  airflow, airflow setpoint, radiator valve
  position data for all zones

output: clusters of zones based on  temperature
and airflow control error

for i = 1 to 8
  method: {k-means, hierarchical, GMM}
  for j = 1 to 3
    execute cluster analysis Zi with method j
    compute Calinski-Harabasz index
  select clustering method
  cluster zones
  flag abnormal clusters
```

```
procedure: temporal clustering for AHU data

input: outdoor and return air dampers, heating
  and cooling coils, humidifier, heat recovery
  wheel, supply fan, radiator valve positions,
  return, supply, and outdoor temperatures,
  return air humidity, supply air pressure data

output: clusters of operation periods based on
  actuator and sensor behaviour

for i = 1 to 4
  method: {k-means, hierarchical, GMM}
  for j = 1 to 3
    execute cluster analysis Si with method j
    compute Calinski-Harabasz index
  select clustering method
  cluster operation periods
  flag clusters with abnormal actuator and
  sensor behaviour
```

Fig. 2. Pseudocodes presenting the procedure for the cluster analysis-based method.

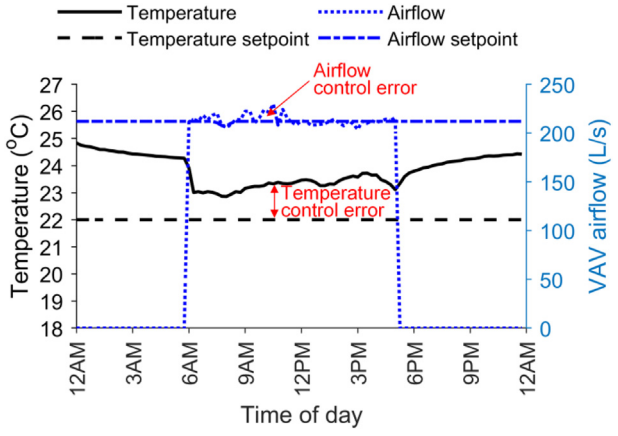

Fig. 3. An illustrative example for the airflow and temperature control errors.

to be identified by the operations staff. Alternatively, Z2 can be applied on data from all zones to group them based on their control error patterns with respect to the outdoor temperature. After employing a min–max feature scaling, the two parameters of the line-fit (intercept and slope) are clustered. Note that the min–max feature scaling is applied to the two parameters of the line-fits (not on the outdoor temperature and temperature control error data) to ensure that intercept and slope parameters account for equal importance in clustering. With this analysis, zones can be grouped into three categories: zones in which the mean absolute temperature control error increases, decreases, and does not change with increasing outdoor temperature.

In steps three to six (Z3 to Z6 in Table 1), daily variation patterns of temperature and airflow control errors are investigated. Specifically, Z3 and Z5 group mean weekday temperature and airflow control error profiles during December, January, and February, respectively, whereas Z4 and Z6 do the same during June, July, and August. Each of these four involves 24 hourly values – average hourly temperature or airflow control errors on weekdays. Because the features used are generated from a single data point type (temperature or airflow control error), a min–max feature scaling is not applied.

The last two steps of zone-level anomaly detection (Z7 and Z8) are intended to identify actuators that do not respond to temperature control error as expected. To this end, as in the example shown in Fig. 4, for each zone, two logistic regression models with four parameters each (two to define the sigmoid shape and two for min–max scaling) are trained between temperature control error and airflow rate and between temperature control error and radiator state. The parameters of regression models are estimated with the genetic algorithm by minimizing the misfit between the data and the model. The parameter estimates (a, b, c, d in Fig. 4) are confined to the physically meaningful range – i.e., non-negative parameter values for a and b, a positive value for d with airflow and a negative value for radiator. After applying a min–max scaling to the parameter estimates a, b, c, and d, the clustering algorithms are applied to identify distinct airflow and radiator valve response

Table 1
Intermediate steps (Z1 to Z8) of the zone-level cluster analysis-based anomaly detection.

Cluster analysis	Feature description	Feature post-processing	Algorithms	Number of clusters	Application
Z1	Mean absolute temperature and airflow control error during workhours(two features per zone)	Workhours Normalized [0,1]	• k-means with squared Euclidean distances • Hierarchical clustering with Ward's linkage method using Euclidean distances • GMM clustering	2 to 10 clusters	Isolate zones with large airflow and temperature control errors
Z2	Slope and intercept of a line-fit between indoor temperature control error and outdoor temperature(two features per zone)	Workhours Normalized [0,1]			Interpret the relationship between temperature control error and outdoor temperature
Z3	Mean weekday temperature control error(24 features per zone)	December, January, February			Identify daily variation patterns of temperature control error in different zones
Z4		June, July, August			
Z5	Mean weekday airflow control error(24 features per zone)	December, January, February			Identify daily variation patterns of airflow control error in different zones
Z6		June, July, August			
Z7	Four parameters of a logistic regression fit between the temperature control error and the airflow rate (as explained in Fig. 4.a)(four features per zone)	Workhours			Identify zones with abnormal airflow control
Z8	Four parameters of a logistic regression fit between the temperature control error and the radiator valve position (as explained in Fig. 4.b)(four features per zone)				Identify zones with abnormal radiator control

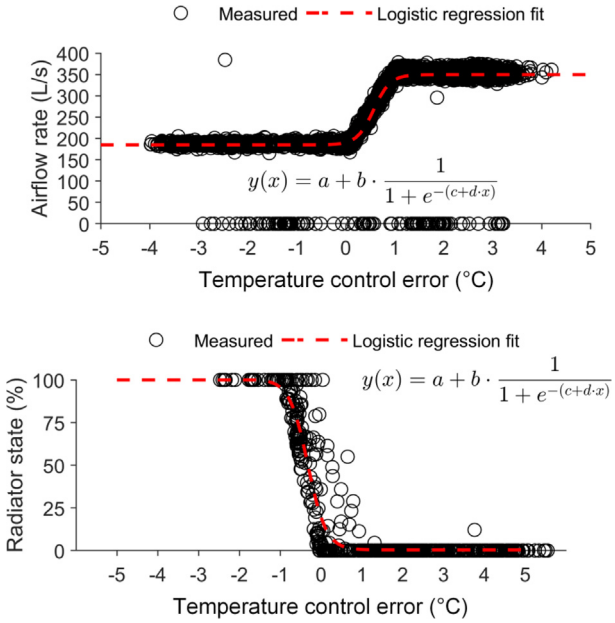

Fig. 4. A logistic regression fit between (a) temperature control error and airflow rate and (b) temperature control error and radiator valve state in a thermal zone.

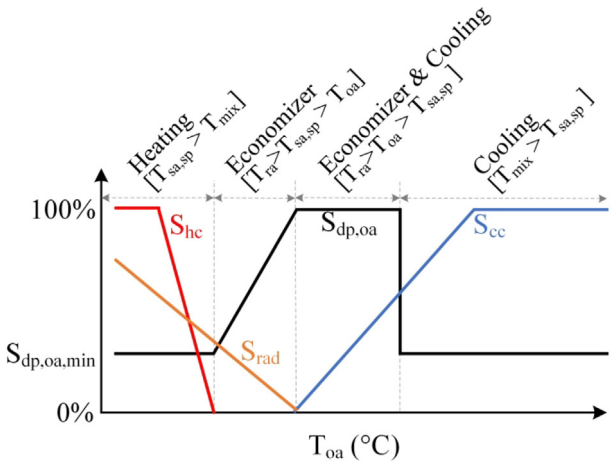

Fig. 5. The four modes of operation of a typical AHU and the expected control signal for actuators.

patterns subject to deviations from the temperature setpoints. It is important to note that Z7 and Z8 can only be applied to zones that experience fluctuations above and below the temperature setpoint throughout the year. If a zone's temperature does not vary throughout the year, the logistic regression model shown in Fig. 4 cannot be developed. So, the genetic algorithm-based parameter estimation is applied to zones that exhibit at least a ± 1 °C variation from the setpoint.

2.2.2. AHU-level anomaly detection

As illustrated in Fig. 5, a properly configured AHU's operation can be grouped into four different modes, heating, economizer, economizer with cooling, and cooling:

- In the heating mode, the mixed air temperature T_{mix} (when the outdoor damper is at the minimum position setpoint) is less than the supply air temperature setpoint $T_{sa,sp}$. Thus, $S_{dp,oa}$ is kept at a position adequate to maintain the ventilation requirements (i.e., the minimum damper position), S_{hc}, S_{hrw}, S_{rad}, and S_h are expected to be greater than zero, and T_{sa} should be higher than $\frac{S_{dp,oa}\cdot T_{oa}+S_{dp,ra}\cdot T_{ra}}{S_{dp,oa}+S_{dp,ra}}$.
- In the economizer mode, the outdoor temperature T_{oa} is less than the supply air temperature setpoint $T_{sa,sp}$, whereas the return air temperature T_{ra} is higher than the supply air temperature setpoint $T_{sa,sp}$. The cooling needs can be entirely offset by simply increasing outdoor air fraction. Thus, $S_{dp,oa}$ is modulated between the minimum damper position setpoint and 100%, and S_{hc}, S_{cc}, S_{hrw}, and S_h are expected to be zero. While it is normal that a few zones require perimeter heating in the economizer mode (e.g., North-facing spaces with low occupancy), the fraction of active perimeter heating devices S_{rad} should be very low. High S_{rad} values in the economizer mode is likely due to low supply air temperature setpoints $T_{sa,sp}$ triggering simulta-

neous perimeter heating and free cooling. And, the problem can be resolved by $T_{sa,sp}$ reset strategies based on the outdoor temperature or the number of zones that require cooling. Further information on $T_{sa,sp}$ reset strategies can be found in ASHRAE Guideline 36 [50]. In the economizer mode, neglecting the impact of temperature rise across the supply fan, T_{sa} should be approximately equal to $\frac{S_{dp,oa} \cdot T_{oa} + S_{dp,ra} \cdot T_{ra}}{S_{dp,oa} + S_{dp,ra}}$.

- In the economizer mode with cooling, the outdoor temperature T_{oa} is less than the return air temperature T_{ra}, while it is higher than the supply air temperature setpoint $T_{sa,sp}$. Hence, the cooling needs can be partly offset by completely opening the outdoor damper. Thus, $S_{dp,oa}$ should be fully open, and S_{cc} should be greater than zero, whereas S_{hc}, S_{hrw}, S_{rad}, and S_h should be zero. T_{sa} is expected to be less than T_{oa}.
- In the cooling mode, the outdoor temperature T_{oa} is above the return air temperature T_{ra}. Thus, $S_{dp,oa}$ should be at the minimum damper position setpoint $S_{dp,oa,min}$, S_{cc} should be greater than zero, and S_{hc}, S_{hrw}, S_{rad}, and S_h should be zero. T_{sa} is expected to be less than $\frac{S_{dp,oa} \cdot T_{oa} + S_{dp,ra} \cdot T_{ra}}{S_{dp,oa} + S_{dp,ra}}$.

Note that the term $\frac{S_{dp,oa} \cdot T_{oa} + S_{dp,ra} \cdot T_{ra}}{S_{dp,oa} + S_{dp,ra}}$ implicitly approximates the mixed air temperature. While this linear approximation can underestimate the outdoor air fraction by as much as 20% at outdoor damper positions less than 30% [49], our intent here is not to develop a model for the mixed air temperature. This approximation is intended merely as a benchmark value to identify unreasonable operating conditions. Note that this benchmark value would not provide a meaningful insight if the heating and cooling coils are simultaneously available. The text explaining the four modes of operation neglects the effect of latent heat for the ease of interpretation. When there is a substantial difference in the humidity ratio of the return and outdoor air, the term temperature should be replaced with the enthalpy of these air streams.

In four steps, the AHU-level anomaly detection method applies cluster analysis on BAS data from an AHU, identifies deviations from these four modes of operation, and helps interpret causes of these deviations (see Table 2).

The first step (S1 in Table 2) involves clustering daily weekday profiles of five data point types pertaining to an AHU (outdoor air damper, HRW state, heating and cooling coil state, and fraction of perimeter heaters on). By using the hourly mean weekday profiles for these five data point types (120 features for each weekday), days with similar AHU operation are grouped together. This step is intended to reveal abnormal AHU operation periods and to detect deviations from the intended sequence of operation. Further, as typical daily actuator responses in lieu of typical instantaneous actuator responses are clustered, cross-correlative anomalies such as cooling or economizing a few timesteps after heating can be revealed with this analysis. Note that min–max feature scaling is not employed in S1 because all actuators are analog outputs taking values between 0 and 100.

In addition to the five data point types used in S1, the second step (S2 in Table 2) also uses three sensor data point types: outdoor, return, and supply air temperatures. Hourly measurements for these eight data point types during workhours are normalized with min–max feature scaling and clustered. Through this step, one can not only identify operational anomalies but also interpret their potential causes by looking at outdoor, return, and supply air temperatures.

The third step (S3 in Table 2) employed clustering on hourly outdoor temperature, return air temperature, and outdoor damper position during workhours normalized with min–max feature scaling. Mean and standard deviations of the sensor and actuator measurements at instances of each cluster are reported. Step three is intended to reveal distinct modes of operation of the outdoor air damper at different indoor and outdoor conditions.

In addition to the eight data point types used in S2, the fourth step (S4 in Table 2) uses min–max normalized hourly data from three actuators and two sensors: return air damper, humidifier valve state, supply fan state, return air humidity, and supply air pressure during workhours. Considering the large number of data point types and their functional relationships, a dimensionality reduction technique, the principal component analysis (PCA), is employed prior to clustering. The PCA scores for the principal components explaining 95% of variability are used with clustering. The median of the sensor and actuator measurements at instances of each cluster is computed and displayed on a typical AHU schematic. Step four is intended to present an overview of the distinct operational modes of an AHU.

2.3. BAS data for the case study

The cluster analysis-based method at the zone-level was demonstrated with a zone-level dataset from a large office building occupied by government employees in Ottawa, Canada. The building's floor area is approximately 45,000 m^2. It was originally built in 1952; the HVAC equipment and control infrastructure were retrofitted at multiple stages between 2008 and 2012. The building was connected to a district plant that continuously supplied steam and chilled water to 17 buildings (including the building of this study) year-round. To employ steps Z1 to Z8 listed in Table 1, the energy management system of the building was queried. In total, data from 247 VAV zones were downloaded from Jan 1, 2018 to Dec 31, 2018 at 60-min intervals. Of them, 58 contained hydronic perimeter heaters. Table 3 presents an overview of the dataset used for the anomaly detection method at the zone-level. It is important to note that the building contained more than 247 VAV zones. We did not include data from a few zones in our analysis due to data quality issues. The data collection in these zones was either interrupted for more than 24 h or the sensor readings were unexpectedly stagnant continuously for more than 24 h.

The anomaly detection method (S1 to S4) at the AHU-level was demonstrated with a dataset from an academic office building in Ottawa, Canada. The building's floor area is approximately 6,000 m^2. It was constructed in 2011. The building was connected to a district heating plant serving all campus buildings and there were chillers serving this building specifically. Heating was available from October to April, whereas cooling was available from May to September. There were two identical AHUs in this building; we randomly selected one of them for this study. In this building, every zone was equipped with a ceiling-mounted hydronic perimeter heating device and/or a VAV reheat coil. Note that in this paper the term perimeter heating devices represent both hydronic perimeter heaters and VAV reheat coils. The data from this AHU were downloaded from Jul 1, 2017 to Jun 30, 2018 at 60-min timesteps. Table 4 presents an overview of the AHU dataset.

3. Results and discussion

This section presents the results from the case study to demonstrate the cluster analysis method. The potential underlying issues leading to these anomalies were interpreted and, when it was possible, verified. The limitations of the methods were identified, and future work recommendations were developed.

3.1. Zone-level anomalies

Fig. 6.a presents the cluster analysis results for mean absolute airflow and temperature control errors (Z1 in Table 1). For Z1,

Table 2
Intermediate steps (S1 to S4) of the system-level cluster analysis.

Cluster analysis	Feature description	Feature post-processing	Algorithm	Number of clusters	Application
S1	Daily weekday profiles for outdoor damper, HRW state, heating and cooling coil state, and fraction of perimeter heaters on(120 features per day for 5 data point types × 24 h)	Weekdays	• k-means with squared Euclidean distances • Hierarchical clustering with Ward's linkage method using Euclidean distances • GMM clustering	2 to 10 clusters	Identify day types with distinct hourly actuator profiles
S2	Hourly outdoor damper, HRW state, heating and cooling coil state, fraction of perimeter heaters on, outdoor, return, and supply air temperatures(8 features)	When the supply fan is operational Normalized [0,1]			Identify unique operational patterns and explore causality
S3	Hourly outdoor damper, return air temperature, outdoor temperature(3 features)				Identify unique operational patterns for AHU outdoor damper
S4	Hourly outdoor damper, HRW state, heating and cooling coil state, fraction of perimeter heaters on, supply fan state, return air damper, humidifier state, outdoor, return, and supply air temperatures, return air humidity, and supply air pressure(13 features)	When the supply fan is operational Principal component analysis (PCA) scores explaining 95% of the variability			Identify unique operational patterns and interpret abnormalities

Table 3
An overview of the data used to demonstrate the method for zone-level anomalies.

Interval data	Number of zones	Data point types
from Jan 1, 2018 to Dec 31, 2018 at 60-min timesteps	247 (189 without perimeter heaters and 58 with perimeter heaters)	Indoor temperature (°C) Indoor temperature setpoint (°C) Airflow rate (L/s) Airflow setpoint (L/s) Perimeter heater state (%)

Table 4
An overview of the data used to demonstrate the method for system-level anomalies.

Interval data	Sensor data	Actuator data
from Jul 1, 2017 to Jun 30, 2018 at 60-min timesteps	Outdoor temperature (°C) Return air temperature (°C) Return air humidity (%) Supply air temperature (°C) Supply air pressure (Pa)	Outdoor air damper position (%) Return air damper position (%) HRW state (%) Heating coil state (%) Cooling coil state (%) Humidifier state (%) Supply fan state (%) Fraction of perimeter heaters on (%)

the k-means algorithm with four clusters maximized the Calinski-Harabasz index. We identified two clusters with anomalies: Z1C1 for zones with large mean absolute temperature control error (n = 28) and Z1C2 for zones with large mean absolute airflow control error (n = 8). Three likely issues associated with zones in cluster Z1C2 are faulty airflow sensors (i.e., differential pressure sensors), faulty dampers that stuck at a certain position, and inappropriate airflow setpoints. In all cases, the appropriate action is to dispatch a technician to inspect these VAV units.

To better understand the underlying issues leading to the high mean absolute temperature control error in Z1C1, we trained a line-fit between the outdoor temperature and the indoor temperature control error for the 28 zones of Z1C1 (Fig. 6.b). Subsequently, we clustered them by looking at the slope and intercept parameters of each line-fit as described in Z2 in Table 1. For Z2, we identified that the k-means algorithm with three clusters maximized the Calinski-Harabasz index. In two of the 28 zones with high mean absolute temperature control error, absolute temperature control error was found to increase with decreasing outdoor temperatures (Z2C3). Given that these zones do not receive adequate heating, the appropriate action is to assign a technician to inspect the perimeter heating systems. In contrast, seven zones identified within Z2C1 experienced greater temperature control errors at higher outdoor temperatures. It is likely that these perimeter zones received inadequate airflow due to low airflow setpoints or inappropriately sized VAV units. Nineteen of the 28 zones experienced temperatures persistently 3 °C to 4 °C above the setpoint (Z2C2). This can be interpreted as that these spaces did not receive adequate airflow for cooling or the supply air temperature was too high.

For Z3 to Z6 in Table 1, the hierarchical clustering algorithm with five clusters maximized the Calinski-Harabasz index (see Fig. 7 and Fig. 8). Fig. 7.a presents the cluster analysis results for mean weekday temperature control error during winter (Z3 in Table 1). The analysis identified ten zones (Z3C1) with temperatures 3 to 4 °C lower than the setpoint during workhours. Three of the ten zones also experienced temperatures colder than the setpoints during the summer months (members of Z3C3 in Fig. 7.b). Thus, it is likely that these three zones suffer from excessive minimum airflow rates, which affect the temperature control in both seasons. Admittedly, the solution to this problem is nontrivial. Reducing the minimum airflow setpoints of the VAV terminals may violate the indoor air quality standards, if the zone is used at its design capacity. Increasing the AHU supply air temperature setpoint may cause discomfort in other zones and increase the fan power. Appropriate actions include inspecting zone occupancy levels and deploying CO_2 sensors for demand control ventilation to reduce minimum airflow rates or tuning the supply air temperature setpoints after ensuring that doing so does not cause discomfort to other zones. For the remaining seven zones of Z3C1 in Fig. 7.a, temperatures colder than the setpoint during the winter can be attributed to faulty or undersized perimeter heaters.

Fig. 7.b presents the cluster analysis results for the mean weekday temperature control error during the summer (Z4 in Table 1). The analysis points out 24 zones with temperatures over 4 °C higher than the setpoint during workhours. Eleven of them were members of Z6C2 in Fig. 8.b, meaning that they were able to main-

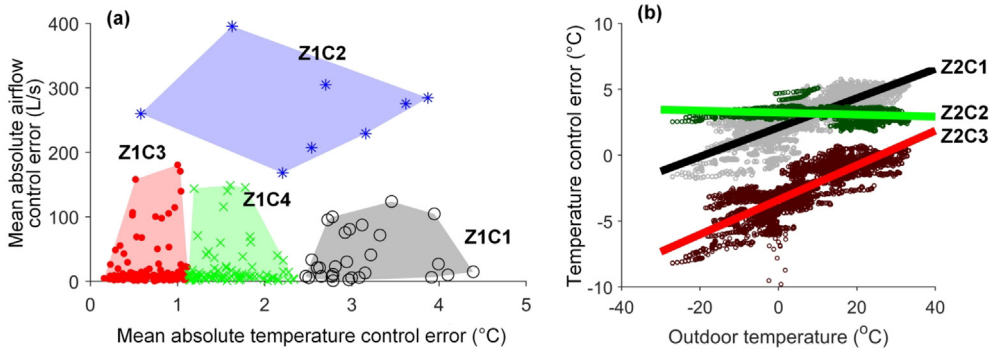

Fig. 6. Clustering (a) the mean absolute temperature and airflow control error (see Z1 in Table 1) and (b) the slope and intercept of a line-fit between indoor temperature control error and outdoor temperature for the zones with large mean absolute temperature control error (see Z2 in Table 1).

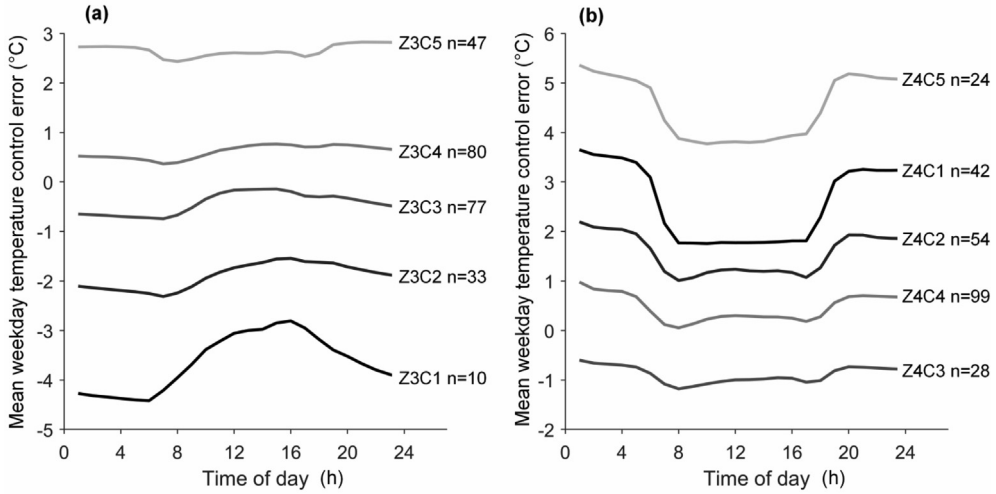

Fig. 7. Clustering the mean weekday temperature control error profiles for (a) winter (see Z3 in Table 1) and (b) summer (see Z4 in Table 1). The number of zones (n) identified within each cluster is also annotated in the figure. Note that control error profiles present the mean for each cluster.

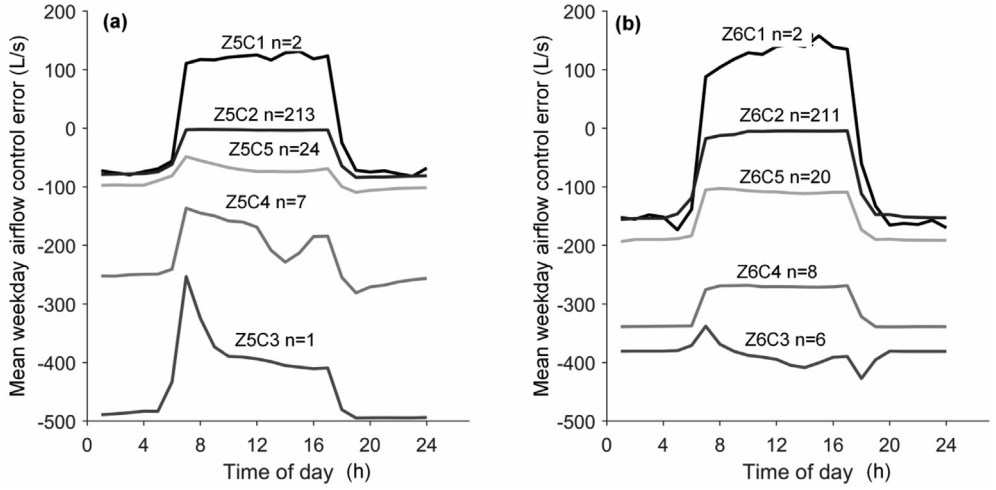

Fig. 8. Clustering the mean weekday airflow control error profiles for (a) winter (see Z5 in Table 1) and (b) summer (see Z6 in Table 1). The number of zones (n) identified within each cluster is also annotated in the figure. Note that control error profiles present the mean for each cluster.

tain the predefined airflow setpoint. Thus, high mean weekday temperature control error in these zones can be attributed to inadequate airflow setpoints or undersized VAV terminal units. The remaining 13 zones of Z4C5 in Fig. 7.b were members of the clusters that experience low airflow in Fig. 8.b (Z6C3, Z6C4, Z6C5). Therefore, the summertime overheating in these zones can be attributed to faulty VAV dampers obstructing the airflow to these zones. Lastly, the two zones in Z5C1 of Fig. 8.a and Z6C1 of Fig. 8.

b were identical. When the AHU supply fan turns on, these two zones appeared to receive more airflow than the setpoint. This anomaly can be attributed to a potential damper stuck open fault.

Fig. 9 presents the cluster analysis results for the zone-level logistic regression models predicting the airflow rate as a function of the temperature control error. Recall that the models were developed as described in Table 1 (Z7), and the number of clusters were selected by calculating the Calinski-Harabasz index over a range of clusters with different clustering algorithms. Through this process, we selected the k-means algorithm with four clusters for Z7. Note that only 168 of the 247 zones exhibit a ± 1 °C variation across the temperature setpoint throughout the year. The temperatures in the remaining zones were relatively constant; thus, logistic regression models could not be developed for these zones with the data available. Among the 168 zones for which a logistic regression model could be developed, the airflow rate in 17 did not change with respect to the temperature control error. This can be attributed to faulty VAV dampers or airflow sensors.

Fig. 10 presents the cluster analysis results for the logistic regression models predicting the radiator position as a function of the temperature control error (Z8 in Table 1). For Z8, the k-means algorithm with three clusters was selected. Note that the models could be developed for 56 of the 58 zones with a radiator. This is because the temperatures in the remaining two zones were mostly time-invariant in our dataset. In these two zones, the difference between the warmest temperature was less than 1 °C higher than the setpoint and the coldest temperature was less than 1 °C lower than the setpoint. In three of the 56 zones, the radiator valves did not open as expected when the temperatures were lower than the setpoint. This can be attributed to faulty radiator valve actuators. Note that these three zones did not experience an anomaly related with the temperature control during workhours – which could be detected through analysis steps Z1 to Z4. Similarly, five of the 17 zones detected with an abnormal airflow response in Fig. 7 were not detected in any other analysis step. Therefore, investigation of the response of radiator valves and airflow rates with the temperature control error in Z7 and Z8 could provide complementary insights to Z1 to Z6. In the case of Z7, the benefit of the cluster analysis was to consolidate a dataset of 168 zones × 8760 h to four logistic regression curves with four parameters each. Similarly, the cluster analysis with Z8 consolidated a dataset of 56 zones × 8760 h to three logistic regression curves with four parameters each – facilitating the process of discovery of abnormal operational behaviours by an energy manager or an operator.

Fig. 11 presents an overview of the anomalies detected through different clustering approaches. In total, 126 anomalies were discovered in 77 zones. Simply put, at least one anomaly was detected in over 30% of the 247 zones of this study. This observation highlights the prevalence of zone-level anomalies such as zones that cannot meet temperature and airflow setpoints due to faulty VAV airflow sensors, dampers, perimeter heaters, and inappropriate airflow setpoints. While the method cannot diagnose the root-causes of the anomalies, it broadly helps interpret whether the problem is arising from a VAV unit or a perimeter heater. Note that in general anomalies in engineering systems are rare events – thus anomaly detection algorithms are often designed for the detection of rare events. However, the results from this case study demonstrate that zone-level anomalies in old office buildings can be widespread and can detrimentally affect comfort and energy performance.

3.2. AHU anomalies

Fig. 12 presents the results of the cluster analysis to identify distinct daily AHU operation modes (see S1 in Table 2). The k-means algorithm with three clusters was selected for S1. Through this analysis, we identified three unique day types. One of them (S1C1 in Fig. 12) represents 7% of the workdays. During this period, the average outdoor temperature was −13 °C. The average outdoor damper position was about 25% during the day, and it correctly shuts down overnight. The heating coil appeared to be used at relatively low actuation levels overnight, whereas the HRW was infrequently operational during the day.

The second day type (S1C2 in Fig. 12) represents 52% of the year. During this period, the average outdoor temperature was 0 °C, the heating and cooling coils and the HRW were not operational, and over 50% of the radiators were on throughout the day. Even though over 50% of the zones require heating, the average outdoor damper

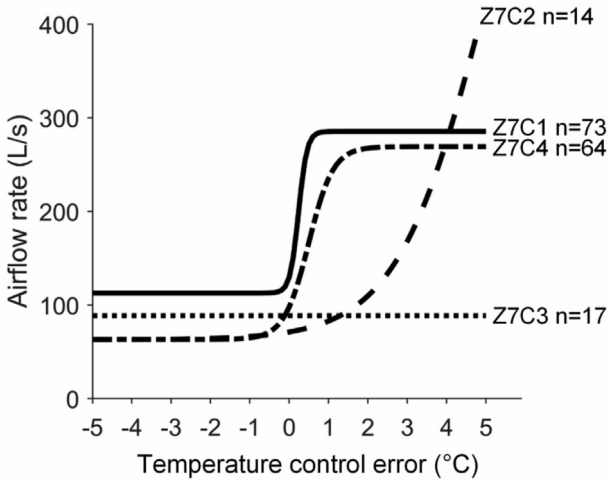

Fig. 9. Typical airflow rate response profiles with respect to the temperature control error (see Z7 in Table 1 and Fig. 4.a). The number of zones (n) identified within each cluster is also annotated in the figure. Note that the total number of zones in the figure is 168 which is less than the 247 zones of this study. A logistic fit could not be trained for the remaining 79 zones as these zones were always above or always below the temperature setpoint year-round.

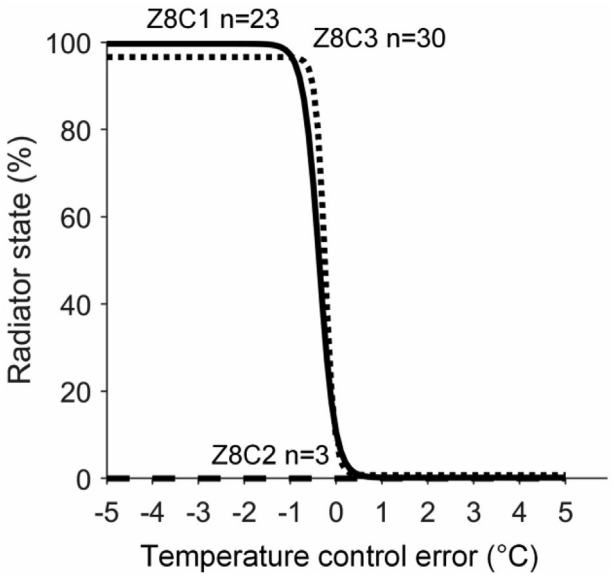

Fig. 10. Typical radiator valve response profiles with respect to the temperature control error (see Z8 in Table 1 and Fig. 4.b). The number of zones (n) identified within each cluster is also annotated in the figure. Note that the total number of zones in the figure is 56 which is less than the 58 zones of this study with perimeter heating. A logistic fit could not be trained for two of the zones as these zones were always above or always below the temperature setpoint year-round.

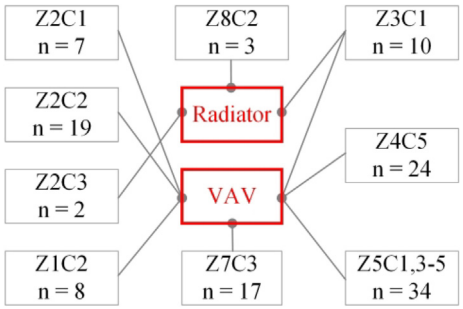

Fig. 11. Summary of zone-level anomalies detected in Figs. 6 to 10 (Z1 to Z8) and their association with VAV terminal units and perimeter heaters. The number of anomalous zones (n) identified by each analysis step is also annotated in the figure.

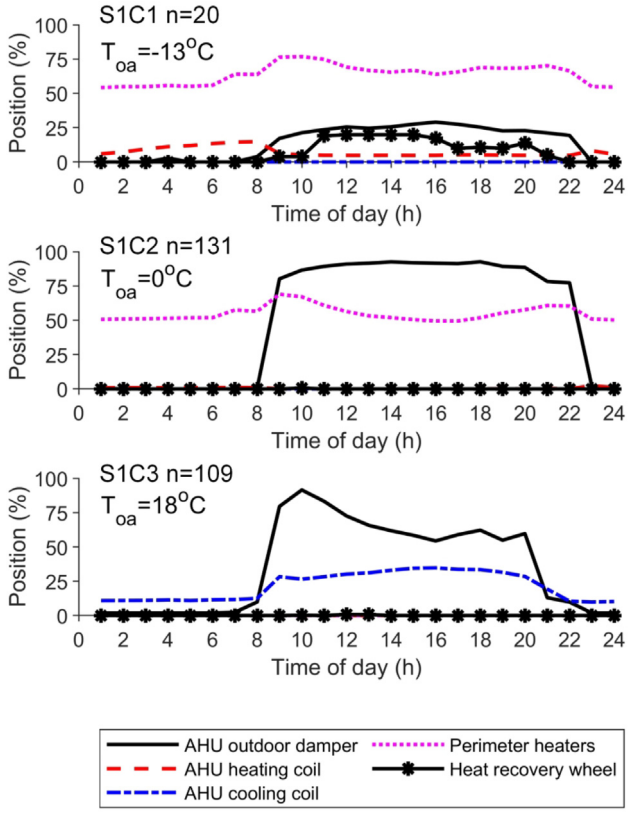

Fig. 12. Distinct daily AHU actuator profiles (see S1 in Table 2). The character n represents the number of days in each cluster.

position was 80%; in other words, the AHU was operating in the economizer mode while many of the zones required heating. While it is, to a certain extent, inevitable to have some overlap between the perimeter heating use and the economizer mode due to differences in space heating and cooling demand in individual zones, excessive use of the perimeter heating devices in the economizer mode is often a result of inappropriately low supply air temperature setpoints in the heating season [51]. And, it can be largely eliminated through a supply air temperature setpoint reset strategy based on outdoor temperature or the number of zones that require cooling [50].

The third day type (S1C3 in Fig. 12) represents 41% of the year, during which the outdoor temperature was on average 18 °C, the heating coil, radiators, and HRW were not operational. In the morning, the outdoor damper and cooling coil were at 90% and 25% open position, respectively – as expected with the economizer during cooling mode. In the afternoon, both the damper and the cooling coil were at about 40% open position, respectively – as expected during the cooling mode.

To interpret the outdoor damper operation behaviour in S1C2 of Fig. 12, the cluster analysis S2 in Table 2 was conducted with hourly sensor and actuator data during normal workhours. For S2, we identified that the k-means algorithm with six clusters maximize the Calinski-Harabasz index. The parallel coordinates plots shown in Fig. 13 present six clusters representing six unique operating conditions. The results indicate that the largest cluster (S2C1) represents 47% of the dataset. In cluster S2C1, the average outdoor damper position was 93%, the average outdoor temperature was 1 °C, 55% of the radiators were operational, and the return air temperature was 22.0 °C. In contrast, in cluster S2C2 (which represents 7% of the dataset), the outdoor damper was at 25% open position, while the return air temperature was 21.8 °C. Similarly, in clusters S2C4 and S2C5, the return air temperature was 22.2 °C and 24.0 °C, respectively; in both cases, the AHU outdoor damper was mostly open at 98% and 84% positions. At outdoor temperatures higher than 20 °C, the outdoor damper was at 50% open position. The outdoor and exhaust air dampers were fully closed when the heating coil and the HRW were operational. Recirculation with return air only can happen during the warm-up periods prior to occupancy; however, when this happens, the HRW does not need to operate – because there is no exhaust air to recover heat from nor outdoor air to preheat. In other words, this observation highlights an anomaly as HRW is a device intended to preheat the cold outdoor air by extracting heat from the exhaust air; thus, when it operates, the outdoor damper should be open for ventilation purposes. Further, the HRW and heating coil were used in only two percent of the dataset (S2C6 in Fig. 13). Based on the results of this cluster analysis, one can interpret that the economizer mode increases outdoor airflow when the return air temperature was greater than 22 °C, the outdoor temperature was less than 20 °C, and the heating coil and HRW were not operational. However, in cluster S2C1, a large fraction of the perimeter heating devices were operating to keep the indoor temperatures above the default temperature setpoint of 22 °C, while the AHU was operating in the economizer mode to maintain an inappropriately low supply air temperature of about 16 °C in the heating season. This anomaly not only led to an increase in the space heating loads but also inhibited the use of the HRW to recover heat from the return air. Note that this energy intensive fault remained undetected for seven years (until this study) despite several *retro*-commissioning exercises, the availability of a commercial FDD tool, and an in-house energy manager.

Fig. 14 presents the cluster analysis results with three features calculated from the outdoor damper position, and outdoor and return air temperatures (see S3 in Table 2). For S3, the GMM clustering algorithm with five clusters was selected. The figure also presents the mean and standard deviation of the heating and cooling coil, HRW, and radiator states. The cluster S3C3 in Fig. 14 corresponds to the problematic mode of operation in which the economizer mode overlaps with the excessive use of perimeter heating devices. Only in S3C2 the heating coil and the HRW were used; while S3C2 represented only 2% of the dataset. Note that S3C2 (Fig. 14) and S2C6 (Fig. 13) correspond to the same operational periods – recirculation with return air only during the warm-up periods prior to occupancy. Because the AHU is scheduled to turn off at night, the AHU heating coil and the VAV reheat coils cannot be used to maintain the zone temperature setpoints. On cold winter mornings captured in S3C2, while ceiling-mounted hydronic perimeter heating devices were adequate to prevent freezing, the return air temperature was as low as 15 °C right after the scheduled start of the AHU.

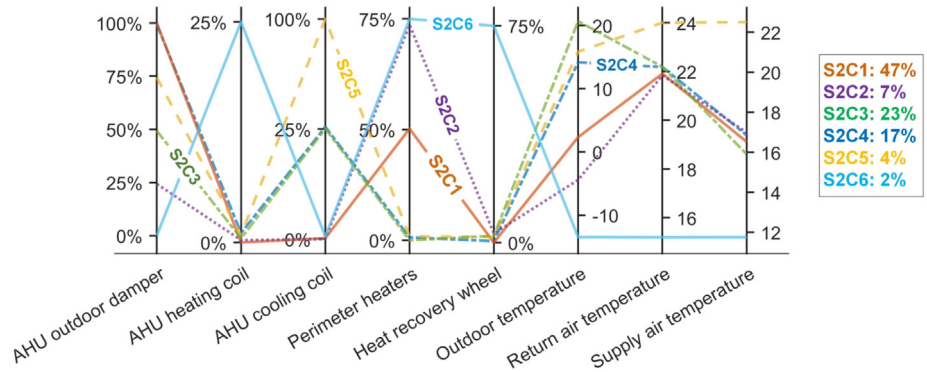

Fig. 13. Typical AHU sensor and actuator response patterns (see S2 in Table 2). Each line represents a different cluster. The outdoor, return, and supply temperatures are shown in degree Celsius. The percentages represent the fraction of instances each cluster represents.

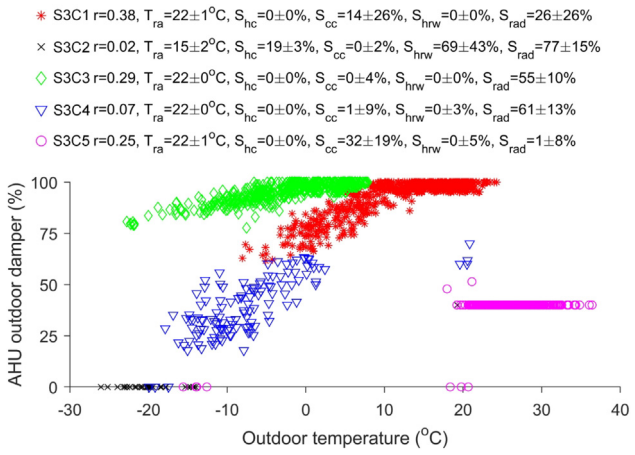

Fig. 14. Typical operating conditions explaining different patterns of AHU outdoor air damper (see S3 in Table 2). The mean μ and standard deviation σ of S_{hc}, S_{cc}, S_{hrw}, S_{rad} in each cluster are also shown in the following form: μ ± σ. The letter r represents the fraction of the operating period of each cluster.

Fig. 15 presents the cluster analysis results for the hourly sensor and actuator data during workhours (see S4 in Table 2). Recall that prior to clustering, the PCA algorithm was used to reduce the dimensionality of the feature space. Thus, the number of features used in clustering was less than the number of sensor and actuator data point types shown in the figure (i.e., 13). For this dataset, we used the scores of the top five principal components in clustering. These principal components accounted for 95% of the variability in the dataset. For S4, the hierarchical clustering algorithm with six clusters was selected. The results of this analysis provide six representative snapshots summarizing distinct operating conditions observed in the dataset. Of these six, the cluster S4C1 accounts for 12% of data. During this period, the heating and cooling coils, the humidifier, and the HRW were mostly off, and the outdoor air damper was completely closed. The fact that the supply temperature was 4 °C lower than return temperature when the average outdoor temperature was −4°C can be attributed to a fault in AHU outdoor dampers not sealing completely.

Another abnormality was noted in S4C3 in Fig. 15. In this period, when the heating and cooling coils, the humidifier, and the

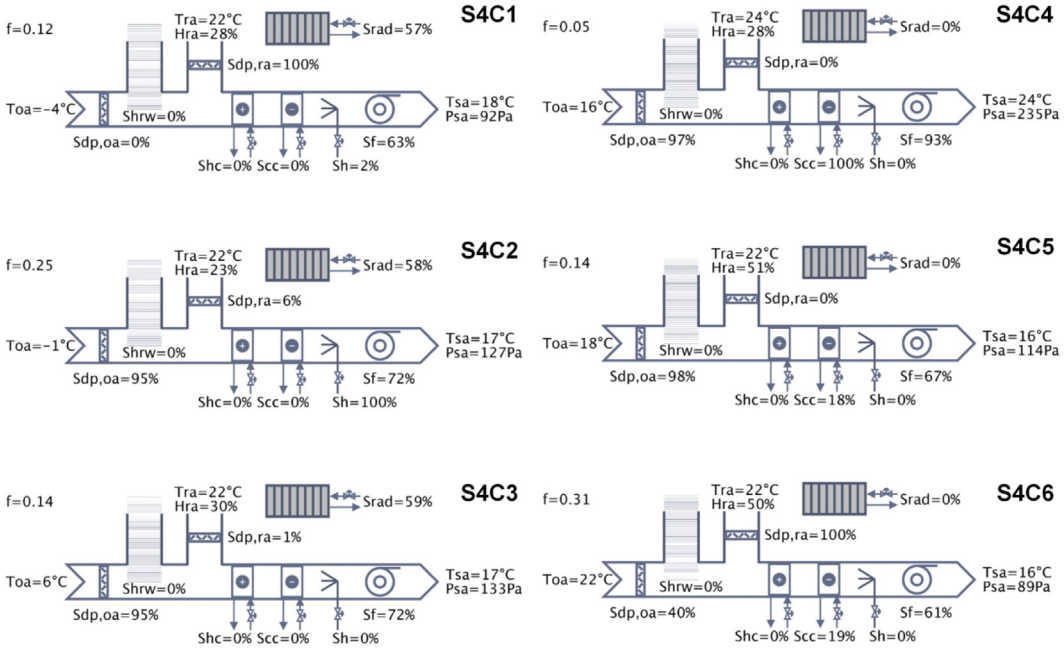

Fig. 15. Distinct operational patterns of the AHU (see S4 in Table 2). Each subfigure represents the median sensor and actuator reading for each of the six clusters. Denoted by character f, the subfigures also include the size of each cluster (i.e., fraction each cluster represents in the dataset).

HRW were off, and the return air damper was nearly closed, the supply air temperature was 11 °C higher than the outdoor temperature. This can be attributed to a leaky return air damper and/or a leaky heating coil valve. In addition, S4C2 and S4C3 highlighted the previously detected anomaly regarding simultaneous economizing while the majority of perimeter heaters were on.

The clusters S4C4 and S4C5 both present an overview of the conditions during the economizer with cooling mode. However, unlike S4C5, S4C4 represents a period in which the two chillers serving the building were not operational. Recall that the chillers serving this building was operational from May to September only, and space heating was available only from October to April. Thus, although the cooling coil valve was open, the cooling coil valve position did not contribute to the control of the supply air temperature. Regardless of the cooling coil valve position, the supply air temperature in S4C4 was 8 °C higher than the outdoor air temperature. Considering that the return air damper was fully closed and the outdoor air damper was fully open, this 8 °C rise in temperature can be largely attributed to the leakage through the return air damper.

Analysis of the findings presented in S4C5 and S4C6 also confirm our previous observations with S4C3 and S4C4 – that the AHU likely has a leaky return air damper. In S4C6, when the average return and outdoor temperatures were both 22 °C and the cooling coil valve was at the ~ 20% open position, the supply temperature was 16 °C – i.e., ~6°C reduction from the expected mixed air temperature to the measured supply air temperature. In S4C5, when the average outdoor temperature was 18 °C, the return damper was fully closed, the cooling coil valve was at ~ 20% open position, the supply temperature was again 16 °C – i.e., only a ~ 2 °C reduction from the expected mixed air temperature to the measured supply air temperature.

3.3. Unresolved issues

Several shortcomings regarding the development and demonstration of the anomaly detection method were identified:

- Earlier in the paper, it is argued that the BAS data need to be consolidated to facilitate the operational anomaly detection process. Different ways to conduct cluster analysis with zone- and AHU-level BAS data were introduced. In May 2019, the analysis results were presented to the energy manager and the operator of the building in which the AHU data were collected. Working with the operations staff, some of the operational issues were addressed. For example, the issue regarding the excessive use of perimeter heaters in the economizer mode was addressed by introducing a low outdoor temperature limit of 5 °C for the availability of the economizer mode. While the results identified were also communicated to the energy manager of the building in which the zone-level data were collected, the authors did not have physical access to this building and could not verify the use of these results by the operations staff. We acknowledge this as a limitation due to working with government buildings. Regardless, cluster analysis is proposed as a powerful technique to systematically simplify complex multidimensional data. By no means, is it a substitute to AFDD methods (such as those listed in ASHRAE Guideline 36 [50]), rather it is intended to engage operations staff in the decision-making process. Future work is planned to design and conduct operator interviews to better understand how they interact and visualize BAS data.
- Note that one could explicitly formulate rules to isolate each abnormal operating condition. For example, excessive use of perimeter heating during the economizer mode can be detected by writing a simple Boolean statement to search for periods with outdoor damper position higher than the minimum damper position setpoint when a significant fraction of the perimeter heating systems are on. Similarly, one can write another Boolean statement to search for rooms with high temperature and airflow control error. While searching for explicit rules defining a finite number of distinct fault states would be useful (which is the common approach in AFDD), this requires writing explicit and unique rules for all possible fault conditions, thresholds, and combinations. Cluster analysis offers a complementary approach to automatically identify each unique pattern of operation and enables discovery of anomalies in an unsupervised manner. Simply put, it may lead to the detection of issues that AFDD rules do not cover or at least it can provide context to interpret conditions leading automatically detected issues by AFDD rules. It may also enable more advanced machine learning techniques such as active learning and semi-supervised learning for AFDD.
- The cluster analysis-based method at the zone-level was demonstrated with data from 247 zones in a single building, whereas at the AHU-level, it was demonstrated with data from a single AHU in another building. Despite the promising results from these case studies, larger-scale testing is needed in different building archetypes and AHU configurations.
- Note that the cluster analysis-based anomaly detection procedure presented in this paper is not intended to be administered by building operators. Instead, we envision that elements of this procedure can be incorporated within AFDD systems to automatically consolidate BAS data to a visual form suitable for human interpretation. This is intended to ensure that operators can assess the appropriateness of automatically generated fault alarms as well as to detect otherwise undetected issues. However, we did not study the effect of this cluster analysis-based anomaly detection method on AFDD tools. If we consolidate the BAS data to an easy to understand form and identify a few recurring patterns of operation, can we expect operators and energy managers to identify and interpret abnormal patterns? Is it possible to have a human-in-the-loop approach whereby a domain expert detects abnormal clusters from a small number of clusters as well as interprets the context behind automatically generated alarms by AFDD tools? Future work should seek answers to these questions.
- As new faults emerge, existing faults are addressed, and changes to sequence of operations are made, operational characteristics of a building will change over time. Hence, the results from these cluster analysis algorithms will need to be executed periodically by an AFDD tool with data from a rolling time window. Future work should investigate the appropriate length of data for the effective use of these algorithms.
- The hyperparameters of the intermediate steps in the cluster-based anomaly detection method (Z1 to 8 in Table 1 and S1 to S4 in Table 2) were selected iteratively by assessing their performance for the case study datasets. To this end, for each step, we studied three different algorithms: k-means clustering, hierarchical clustering, and GMM-based clustering. There are other clustering algorithms that we did not study, such as density-based clustering algorithms. Further, we did not study other anomaly detection techniques aside from clustering. Future work should extend this BAS data anomaly detection method beyond clustering such as linear model-based anomaly detection and probabilistic and statistical model-based anomaly detection [48].

4. Conclusions

The cluster analysis-based method that we put forward in this paper was demonstrated with a year's worth of BAS data from

247 thermal zones and an AHU with an HRW. The method consolidated these large datasets and identified clusters that define distinct patterns of operation. Through the inspection of these clusters, we identified several operational anomalies that otherwise were not detected by the commercial FDD tools in-place or overlooked by the operations staff.

At the zone-level, we identified anomalies in 77 of the 247 zones. The anomalies detected were associated with zones that cannot meet temperature and airflow setpoints or to VAV units and perimeter heaters that incorrectly respond to deviations from a temperature setpoint. Although it was not possible to identify the root cause of these anomalies, the cluster analysis helped interpret whether a problem was arising from a VAV unit's damper or airflow sensor, a perimeter heater's valve, or an inappropriately selected airflow setpoint.

At the AHU-level, through the cluster analysis, a few representative operating conditions were identified in the dataset. We discovered three anomalies by comparing these patterns of operation to normal modes of operation. One of these anomalies was a simultaneous economizing and heating problem. This anomaly was caused by a programming mistake that disregarded the state of the perimeter heating devices and looked merely at the differential dry-bulb temperature in deciding whether or not the economizer should be activated. This energy-intensive fault affected 39 to 52% of the total operation period and caused the outdoor air damper to remain fully open and the HRW to remain off during most of the winter. The authors corrected this programming mistake. In addition, two other anomalies associated with leaky return and outdoor air dampers were identified. Future work is planned to carry out operator interviews to assess the appropriateness of the cluster analysis-based method and to monitor energy savings once the faults causing these anomalies are fixed.

CRediT authorship contribution statement

H. Burak Gunay: Conceptualization, Methodology, Investigation. **Zixiao Shi:** Data curation, Formal analysis, Writing - original draft.

Declaration of Competing Interest

The authors declare that they have no known competing financial interests or personal relationships that could have appeared to influence the work reported in this paper.

Acknowledgements

This research is supported by the research funding provided by the Natural Sciences and Engineering Research Council (NSERC) of Canada, Natural Resources Canada, National Research Council Canada, and CopperTree Analytics. The authors acknowledge Dr. Guy Newsham's valuable contributions in preparation of this paper.

Appendix A. Supplementary data

Supplementary data to this article can be found online at https://doi.org/10.1016/j.enbuild.2020.110445.

References

[1] B. Gunay, W. Shen, B. Huchuk, C. Yang, S. Bucking, W. O'Brien, Energy and comfort performance benefits of early detection of building sensor and actuator faults, Build. Serv. Eng. Res. Technol. 39 (2018) 652–666.
[2] B. Dong, Z. O'Neill, Z. Li, A BIM-enabled information infrastructure for building energy Fault Detection and Diagnostics, Autom. Constr. 44 (2014) 197–211.
[3] Z. Shi, W. O'Brien, Development and implementation of automated fault detection and diagnostics for building systems: A review, Autom. Constr. 104 (2019/08/01/ 2019.) 215–229.
[4] W. Kim, S. Katipamula, A review of fault detection and diagnostics methods for building systems, Science and Technology for the Built Environment 24 (2018) 3–21.
[5] Y. Yu, D. Woradechjumroen, D. Yu, A review of fault detection and diagnosis methodologies on air-handling units, Energy Build. 82 (2014/10/01/ 2014.) 550–562.
[6] S. Katipamula, M.R. Brambley, Review Article: Methods for Fault Detection, Diagnostics, and Prognostics for Building Systems—A Review, Part I, HVAC&R Research 11 (2005/01/01 2005.) 3–25.
[7] S. Katipamula, M.R. Brambley, Review Article: Methods for Fault Detection, Diagnostics, and Prognostics for Building Systems—A Review, Part II, HVAC&R Research 11 (2005/04/01 2005.) 169–187.
[8] J. Schein, S.T. Bushby, A hierarchical rule-based fault detection and diagnostic method for HVAC systems, HVAC&R Research 12 (2006) 111–125.
[9] K. Bruton, P. Raftery, P. O'Donovan, N. Aughney, M.M. Keane, D. O'Sullivan, Development and alpha testing of a cloud based automated fault detection and diagnosis tool for Air Handling Units, Autom. Constr. 39 (2014) 70–83.
[10] J. Schein, S.T. Bushby, N.S. Castro, J.M. House, A rule-based fault detection method for air handling units, Energy Build. 38 (2006/12/01/ 2006.) 1485–1492.
[11] J. Schein, J.M. House, Application of control charts for detecting faults in variable-air-volume boxes, ASHRAE Transactions 109 (2003) 671–682.
[12] H. Wang, Y. Chen, C.W. Chan, J. Qin, An online fault diagnosis tool of VAV terminals for building management and control systems, Autom. Constr. 22 (2012) 203–211.
[13] J. Qin, S. Wang, C. Chan, and F. Xiao, "Commissioning and diagnosis of VAV air-conditioning systems," 2006.
[14] S.-H. Cho, H.-C. Yang, M. Zaheer-uddin, B.-C. Ahn, Transient pattern analysis for fault detection and diagnosis of HVAC systems, Energy Convers. Manage. 46 (2005/11/01/ 2005.) 3103–3116.
[15] F. Lauro, F. Moretti, A. Capozzoli, I. Khan, S. Pizzuti, M. Macas, S. Panzieri, Building fan coil electric consumption analysis with fuzzy approaches for fault detection and diagnosis, Energy Procedia 62 (2014) 411–420.
[16] L. Lianzhong, M. Zaheeruddin, Fault tolerant control strategies for a high-rise building hot water heating system, Build. Serv. Eng. Res. Technol. 35 (2014) 653–670.
[17] Z. O'Neill, X. Pang, M. Shashanka, P. Haves, T. Bailey, Model-based real-time whole building energy performance monitoring and diagnostics, J. Build. Perform. Simul. 7 (2014/03/04 2014.) 83–99.
[18] M. Wetter, P. Haves, and B. Coffey, "Building controls virtual test bed," Lawrence Berkeley National Laboratory2008.
[19] S. Wang, Q. Zhou, F. Xiao, A system-level fault detection and diagnosis strategy for HVAC systems involving sensor faults, Energy Build. 42 (2010) 477–490.
[20] M. Yuwono, Y. Guo, J. Wall, J. Li, S. West, G. Platt, S.W. Su, Unsupervised feature selection using swarm intelligence and consensus clustering for automatic fault detection and diagnosis in Heating Ventilation and Air Conditioning systems, Appl. Soft Comput. 34 (2015/09/01/ 2015.) 402–425.
[21] J. Wen and S. Li, "RP 1312: Tools for evaluating fault detection and diagnostic methods for air-handling units," ASHRAE, Ed., ed. Atlanta, US, 2012.
[22] M. Najafi, D.M. Auslander, P. Haves, M.D. Sohn, A statistical pattern analysis framework for rooftop unit diagnostics, HVAC&R Research 18 (2012/06/01 2012.) 406–416.
[23] H. Han, B. Gu, Y. Hong, J. Kang, Automated FDD of multiple-simultaneous faults (MSF) and the application to building chillers, Energy Build. 43 (2011) 2524–2532.
[24] Z. Du, B. Fan, X. Jin, J. Chi, Fault detection and diagnosis for buildings and HVAC systems using combined neural networks and subtractive clustering analysis, Build. Environ. 73 (2014/03/01/ 2014.) 1–11.
[25] B. Fan, Z. Du, X. Jin, X. Yang, Y. Guo, A hybrid FDD strategy for local system of AHU based on artificial neural network and wavelet analysis, Build. Environ. 45 (2010/12/01/ 2010.) 2698–2708.
[26] Y. Zhu, X. Jin, Z. Du, Fault diagnosis for sensors in air handling unit based on neural network pre-processed by wavelet and fractal, Energy Build. 44 (2012) 7–16.
[27] M. Najafi, D.M. Auslander, P.L. Bartlett, P. Haves, M.D. Sohn, Application of machine learning in the fault diagnostics of air handling units, Appl. Energy 96 (2012) 347–358.
[28] F. Xiao, Y. Zhao, J. Wen, S. Wang, Bayesian network based FDD strategy for variable air volume terminals, Autom. Constr. 41 (2014) 106–118.
[29] B. Sun, P.B. Luh, Q. Jia, Z.O. Neill, F. Song, Building Energy Doctors: An SPC and Kalman Filter-Based Method for System-Level Fault Detection in HVAC Systems, IEEE Trans. Autom. Sci. Eng. 11 (2014) 215–229.
[30] Z. Shi, W. O'Brien, Sequential state prediction and parameter estimation with constrained dual extended Kalman filter for building zone thermal responses, Energy Build. 183 (2019/01/15/ 2019.) 538–546.
[31] B. Gunay, W. Shen, C. Yang, Characterization of a building's operation using automation data: A review and case study, Build. Environ. 118 (2017/06/01/ 2017.) 196–210.
[32] Z. Shi, W. O'Brien, B. Gunay, "Building zone fault detection with Kalmnan filter based methods," presented at the eSim 2016, Hamilton, ON, 2016.
[33] H.B. Gunay, W. Shen, G. Newsham, Data analytics to improve building performance: A critical review, Autom. Constr. 97 (2019) 96–109.

[34] L.K. Norford, J.A. Wright, R.A. Buswell, D. Luo, C.J. Klaassen, A. Suby, Demonstration of fault detection and diagnosis methods for air-handling units, HVAC&R Research 8 (2002) 41–71.
[35] K.G. Mehrotra, C.K. Mohan, H. Huang, Anomaly detection principles and algorithms, Springer, 2017.
[36] J.E. Seem, Using intelligent data analysis to detect abnormal energy consumption in buildings, Energy Build. 39 (2007) 52–58.
[37] G. Mavromatidis, S. Acha, N. Shah, Diagnostic tools of energy performance for supermarkets using Artificial Neural Network algorithms, Energy Build. 62 (2013/07/01/ 2013.) 304–314.
[38] J. Ploennigs, B. Chen, A. Schumann, N. Brady, Exploiting Generalized Additive Models for Diagnosing Abnormal Energy Use in Buildings, For Energy-Efficient Buildings, Roma, Italy, 2013.
[39] A. Srivastav, A. Tewari, B. Dong, Baseline building energy modeling and localized uncertainty quantification using Gaussian mixture models, Energy Build. 65 (2013/10/01/ 2013.) 438–447.
[40] D. Jacob, S. Dietz, S. Komhard, C. Neumann, S. Herkel, Black-box models for fault detection and performance monitoring of buildings, J. Build. Perform. Simul. 3 (2010/03/01 2010.) 53–62.
[41] J.Y. Park, X. Yang, C. Miller, P. Arjunan, Z. Nagy, Apples or oranges? Identification of fundamental load shape profiles for benchmarking buildings using a large and diverse dataset, Appl. Energy 236 (2019) 1280–1295.
[42] B. Narayanaswamy, B. Balaji, R. Gupta, Y. Agarwal, Data driven investigation of faults in HVAC systems with Model, Cluster and Compare (MCC), in: in *BuildSys 2014 - Proceedings of the 1st ACM Conference on Embedded Systems for Energy-Efficient Buildings*, 2014, pp. 50–59.
[43] D. Arthur and S. Vassilvitskii, "k-means++: The advantages of careful seeding," in Proceedings of the eighteenth annual ACM-SIAM symposium on Discrete algorithms, 2007, pp. 1027-1035.
[44] R. Yan, Z. Ma, G. Kokogiannakis, Y. Zhao, A sensor fault detection strategy for air handling units using cluster analysis, Autom. Constr. 70 (2016/10/01/ 2016.) 77–88.
[45] E. Novikova, M. Bestuzhev, and A. Shorov, "The Visualization-Driven Approach to the Analysis of the HVAC Data," in Studies in Computational Intelligence vol. 868, ed, 2020, pp. 547-552.
[46] M. Ester, H.P. Kriegel, J. Sander, X. Xu, A density-based algorithm for discovering clusters in large spatial databases with noise, Kdd (1996) 226–231.
[47] T. Caliński, J. Harabasz, A dendrite method for cluster analysis, Communications in Statistics-theory and Methods 3 (1974) 1–27.
[48] C.C. Aggarwal, Outlier analysis, Springer, New York, 2017.
[49] L.G. Felker, T.L. Felker, Dampers and airflow control, American Society of Heating, Refrigerating, and Air-Conditioning Engineers (2009).
[50] ASHRAE, Guideline 36: High performance sequences of operation for HVAC systems, American Society of Heating, Refrigerating and Air-Conditioning Engineers, Atlanta, 2018.
[51] H.B. Gunay, G. Newsham, A. Ashouri, I. Wilton, Deriving sequences of operation for air handling units through building performance optimization, J. Build. Perform. Simul. (2020), https://doi.org/10.1080/19401493.2020.1793221.